INTERNATIONAL JOURNAL OF INTEGRATED ENGINEERING
ISSN: 2229-838X e-ISSN: 2600-7916

IJIE

Vol. 16 No. 9 (2024) 326-338
https://publisher.uthm.edu.my/ojs/index.php/ijie

Modeling of InGaAs/InGaP/GaAs/AlInP/Ge-Based Five Junction Solar Module with Wafer Bonding for Efficiency Improvement

Muhammad Shehram[1], Muhammad Najwan Hamidi[1]*, Aeizaal Azman Abdul Wahab[1], Mohd Khairunaz Mat Desa[1]

[1] *School of Electrical & Electronic Engineering, Universiti Sains Malaysia, 14300 Nibong Tebal, MALAYSIA*

*Corresponding Author: najwan@usm.my
DOI: https://doi.org/10.30880/ijie.2024.16.09.027

Article Info

Received: 3 July 2024
Accepted: 12 September 2024
Available online: 30 December 2024

Keywords

Five junction solar module, wafer bonding, window layer, germanium substrate, efficiency improvement

Abstract

The efficiency of solar photovoltaic (PV) modules is a major area of research as global interest in renewable energy grows. This study presents the design and simulation of a five-junction solar module aimed at significantly enhancing efficiency. Each junction is optimized with unique band gap energies, which are crucial for maximizing the module's performance. Higher band gap energy materials exhibit minimal lattice mismatch, while lower band gap materials present higher mismatches. These are effectively connected using wafer bonding, with AlInP serving as the window layer to further improve efficiency. The electrical performance of the multijunction solar cells is determined by a short-circuit current (J_{sc}) of 3.2/3.0/2.5/2.0/1.8 mA/cm^2 across the band gaps, leading to a total J_{sc} of 12.5 mA/cm^2. The open-circuit voltage (V_{oc}) values for each junction range from 2.45 V to 2.65 V, culminating in an overall V_{oc} of 12.8 V. The module achieves a peak power output of 10.5 W and a fill factor of 90%. Notably, the solar module, utilizing InGaP/InGaAs/GaAs/AlInP/Ge, reaches an efficiency of up to 46.7% with materials having a standard band gap length of 1.5 Å. Germanium (Ge), used as a substrate in the bottom junction, is pivotal in this efficiency improvement. These findings were validated through MATLAB/Simulink simulations, highlighting the potential of multijunction PV modules for high-efficiency solar energy conversion.

1. Introduction

In the current day, solar energy offers a promising way to address energy challenges and produce clean, environmentally friendly power. To increase the effectiveness of solar PV modules, extensive research is being done. Single solar cells have a lower efficiency, according to the available literature. However, by including an additional junction, the efficiency of the PV module can be increased by 3.7%. Aluminium indium phosphide (AlInP) has been used as a window layer to connect all the junctions in five junction solar modules, which reduces current leakage and allows for improved efficiency [1]. The usage of four junction solar modules with wafer bonding is an additional strategy for enhancing the performance of solar PV modules. These modules have a window layer and a bond length of 1.5 Å, which reduce current loss and make use of the entire solar spectrum, yielding an efficiency of 42% [2].

Conventional single-junction solar modules typically achieve efficiencies between 16% and 21%. To enhance efficiency, multijunction solar modules are designed to harness the full spectrum of sunlight by incorporating different materials that are sensitive to distinct wavelengths. III-V junction solar modules further improve PV

efficiency, with advancements reaching maximum performance [3]. These multijunction solar cells are often grown on germanium substrates to maximize efficiency, with designs evolving from four-junction to five-junction configurations. AlInP is used as a window layer in these cells, enhancing performance. AlInP, a semiconductor with a 2.0 eV bandgap, effectively converts photons into electrical energy. It consists of AlP and InP alloys, known for their high-temperature tolerance and excellent optical properties [4].

Direct wafer bonding is employed to connect the five junction solar modules, with a bonding thickness ranging from 20 to 30 micrometers. To optimize the performance of the solar modules, all cells are fabricated on a germanium substrate [5]. The thickness of the wafer bonding helps minimize current loss, as the germanium substrate generates the maximum current. The mobility of charge carriers remains uninterrupted within the germanium-based substrate, and direct wafer bonding enhances the flow of charge carrier mobility [6].

The five junction solar modules' characteristic curve is plotted using the MATLAB/Simulink model. This makes it possible to calculate numerous parameters like J_{sc}, V_{oc}, and output power. For optimal connectivity, it is essential to guarantee a suitable voltage match between the top and bottom cells of the PV modules [7]. Additionally, the solar irradiance's intensity affects how well multijunction PV modules operate. During testing, the five junction solar modules are exposed to 1000W/m^2 of radiation while maintaining a 1.5 Å bond length for every junction. The five junction solar PV modules with appropriate bond energy across all junctions have a high efficiency [8].

The presence of multiple junctions in multijunction solar cells contributes to their exceptionally high theoretical efficiency, resulting in improved performance for multijunction PV modules. It is worth noting that the optimal number of junctions for achieving a balance between efficiency and cost-effectiveness is five or less. As the number of junctions increases, there is a corresponding increase in optical and series connection losses, making five junction solar modules particularly suitable for achieving excellent performance [9]. To further enhance the theoretical efficiency of multijunction PV modules, efforts are made to minimize reflection losses. This is accomplished through the design of an anti-reflecting coating that effectively absorbs light within the 300-1800nm wavelength range, thereby reducing reflections within that specific range [10].

Due to its shorter wavelength, the top layer of multijunction solar modules can collect photons that are emitted sooner. The multijunction modules become more effective as a result. By lowering the recombination rate and raising photon generation, efficiency is further improved. Additionally, the addition of a window layer and enhanced wafer bonding and material thickness increase the efficiency of multijunction PV modules [11]. By lowering photon recombination, the window layer is essential for improving the performance of multijunction solar modules. A GaAs window layer is used in this investigation to increase module efficiency [12].

The process of wafer bonding is employed at room temperature to integrate germanium as a substrate in five junction solar modules. All four junctions are connected through molecular beam epitaxy. The implementation of wafer bonding allows for the arrangement of sub-cells within the multijunction solar modules, resulting in an efficiency increase of up to 42% [13]. The efficiency of multijunction PV modules is also influenced by bond resistance. By utilizing wafer bonding techniques, the bond resistance is minimized, leading to an enhancement in the efficiency of the multijunction PV modules [14].

By utilizing AlInP as a window layer and InGaAs as the back surface field layer, the recombination process of photons is minimized, resulting in the maximum performance of multijunction PV modules. This reduction in recombination leads to an increase in V_{oc}, contributing to improved overall performance [15]. When wafer bonding is conducted under high pressure and elevated temperature, the V_{oc} and fill factors are significantly high. Additionally, maintaining a bond length of 1.5A ensures that the J_{sc} remains constant, while the efficiency of multijunction PV modules increases, thereby meeting future energy demands [16].

At both the cell and module levels, multijunction solar cells are developed and defined in terms of their performance and characteristic curve. In [17], the multijunction PV fabrication process as well as the material properties are discussed. Ge in the bottom cell and InGaAs in the middle cell during the multijunction solar module manufacturing process increase the V_{oc} capacity, while Ge in the bottom cell increases the J_{sc} value for increased efficiency [18].

A key objective for many researchers is to develop high-performance solar cells. The first generation of solar modules, based on silicon, utilized only a narrow spectrum of sunlight and had efficiencies below 20%. To improve this, multijunction solar modules have been designed using materials with varying bandgap energies, optimizing efficiency while minimizing heat loss [19]. Today, multijunction PV modules are gaining popularity due to their higher efficiency and reduced cost per unit of electricity. Their improved performance is attributed to lower resistance, reduced heat loss, and decreased recombination rates in the cells [20].

The presence of an intermediate layer plays a significant role in enhancing the efficiency of multijunction solar cells by improving electrical current conductivity and transparency. In triple junction solar cells, the use of graphene as an intermediate layer alongside InGaP/GaAs/InGaAs results in a notable improvement in module conversion efficiency, with potential gains of up to 30.91% [21]. Specific layers are strategically designed to enhance light absorption and increase photocurrent generation, and the materials used in these layers greatly impact the performance of multijunction solar cells. The interconnected layer serves to establish electrical and

Int. Journal of Integrated Engineering Vol. 16 No. 9 (2024) p. 326-338

optical connections between sub cells in multijunction solar cells, minimizing heat loss. Commonly, polymeric materials or metal oxides are utilized as the interconnected layer [22].

A recent study demonstrated that employing a band gap gradient significantly improves the V_{oc} in Cu(In, Ga)Se_2 and Cu(Zn, Sn)Se_2 thin-film solar cells. A novel band gap region, based on Cd(O, S, Se, Te), was integrated within the same crystal structure, in conjunction with a commercial SnO_2 buffer layer at the junction. This configuration resulted in a system efficiency of 20.03% and a V_{oc} of 0.863V [27]. Silicon heterojunction solar cells have also been designed to enhance PV efficiency by incorporating a P-type doped nanocrystalline silicon layer and a transparent oxide layer with low sheet resistance at the rear junction. This design achieved a power conversion efficiency of 26.81% and a fill factor of 86.59% [28].

In another study on thin-film triple-junction solar cells, AlGaAs/GaAs/GaAsBi with a 1.0 eV dilute bismuth component was analysed. A step-graded buffer layer was introduced to improve the crystalline quality of the absorber, achieving an efficiency of 19.1% under the AM 1.5G spectrum [29]. While the efficiency of PV panels generally increases with the number of junctions, it may decrease if the bottom cell has a low band gap. Enhancing the band gap of the lower junction improves panel performance, with five or fewer junctions being the most economically feasible option [30].

The performance of solar cells has steadily improved by utilizing a broader light spectrum. In recent years, perovskite and organic solar cells have gained significant attention due to their simplified fabrication processes, reduced equipment costs, and economic advantages [31]. A study highlighted perovskite-silicon triple-junction solar cells as a promising next step for achieving higher efficiency in multijunction solar cells at a lower cost. These cells achieved a record-high V_{oc} of over 2.8 V, made possible by using the gas quenching method to deposit the top perovskite layer and connect the perovskite layers [32]. Additionally, dual-junction solar cells, which incorporate III-V semiconductor materials with varying band gaps, improve PV efficiency by better absorbing the solar spectrum, achieving an overall efficiency of 35.15% [33].

A recent study introduced single-junction solar cells with a metasurface layer to enhance performance, achieving an absorption efficiency of 97.86% and a power conversion efficiency of 30.87% [34]. Additionally, anti-reflective coatings were applied to triple-junction gallium-arsenide solar cells to minimize reflection losses and improve absorption, reducing reflectivity to as low as 5.506%. This design, implemented in the window layer, significantly boosted the performance of multijunction solar cells [35]. Another study examined III-V multijunction solar cells under ultra-high concentration conditions, with temperature measurements up to 85°C and a solar concentration of 2200 suns [36]. Research also explored the effects of varying thicknesses in the top and middle cells on overall efficiency, along with power deviations caused by different positions and densities of interface defects [37]. Table 1 summarizes the different types of solar cells reviewed.

This work presents the design of a five-junction solar module aimed at improving solar module efficiency by utilizing the full spectrum of sunlight. Each additional junction absorbs a different portion of sunlight, reducing panel temperature and enhancing efficiency. The proposed PV module comprises five junctions and five layers, optimizing efficiency across the entire solar spectrum. The use of AlInP as a window layer and Ge as a substrate helps achieve maximum fill factor and quantum efficiency while minimizing recombination. These design features make the module more efficient than conventional alternatives. In this design, the interconnected layer of AlInP connects the sub-cells both mechanically and electrically, reducing optical losses and boosting photon generation. The interconnected layer, also known as the window layer, enhances the transparency of the solar cells, allowing for maximum photocurrent generation and increasing the overall efficiency of the five-junction module. Additionally, InGaP/InGaAs/GaAs/AlInP layers are grown on germanium substrates to maximize the efficiency of multijunction solar cells. The germanium-based substrate increases the number of minor charge carriers, reducing recombination and enhancing photocurrent generation, thereby further improving the efficiency of multijunction solar modules

2. Methodology

2.1 Five junction solar modules

By incorporating an additional junction composed of unique materials and properties, the performance of multijunction solar modules is significantly improved. This addition enhances the efficiency of the modules by introducing a junction with a thickness ranging from 10 to 20 μm. Each band gap within the junctions possesses a distinct value. The top junction is designed to absorb shorter wavelengths of light, while the bottom band gap is optimized for capturing higher wavelength spectra. The first junction has an energy level of 1.89 eV, followed by the second junction with an energy level of 1.65 eV, the third junction with 1.45 eV, the fourth junction serving as a window layer with germanium and possessing an energy level of 2.0 eV, and finally, the last band gap is germanium-based with a band gap energy of 0.65 eV. Each band gap is electrically and mechanically connected to the adjacent band gap through tunnel junctions as shown in Fig. 1.

Table 1 *Classification of various solar cell types along with their efficiencies under standard global conditions of AM1.5G spectrum, 1000 W/m² irradiance, and a temperature of 25°C*

Type	Efficiency %	V_{oc} (V)	J_{sc} (mA/cm²)	Fill factor %	Test center	Description
Silicon-Based Solar Cells						
Si (Crystalline)	25.0	0.706	42.70	82.8	Sandia (3/99)	UNSW, p-type PERC [38]
Si (Crystalline)	26.7	0.738	42.65	84.9	AIST (3/17)	n-type rear IBC Kaneka [39]
Si (Amorphous)	10.2	0.896	16.36	69.8	AIST (7/14)	AIST [40]
Si (Monocrystalline)	11.9	0.550	28.72	75.0	AIST (2/17)	AIST [41]
Group III-V Solar Cells						
GaAs	29.1	1.1272	29.78	86.7	FhG-ISC (10/18)	Alta devices [42]
InP	24.2	0.939	31.15	82.6	NREL (3/13)	NREL, Crystalline Cell [43]
Chalcogenide-Based Solar Cells						
CIGS	23.6	0.7671	38.30	80.5	FhG-ISC (1/23)	Evolar/UppsalaU [42]
CdTe	22.3	0.8985	31.69	78.9	NREL (2/23)	First solar [42]
CZTS	11.4	0.7458	21.79	69.9	NPVM (5/23)	UNSW (Cd-free) [42]
Solar Cells with Emerging Materials						
Perovskite	26.0	1.19	26.0	84.0	JET (3/23)	IoS/CAS [42]
Organic	19.2	0.9135	26.61	79.0	NREL (3/23)	SJTU [44]
Dye-sensitized	13.0	1.0396	15.55	80.4	FhG-ISE (10/20)	EPFL [45]
Multijunction Solar Cells						
GaInP/GaAs	39.5	2.997	15.44	85.3	NREL (9/21)	NREL Multiple QW [42] [48]
5 Junction (bonded)	38.8	4.767	9.564	85.2	NREL (7/13)	Spectrolab, 2-Terminal [42]
6 Junction (Monolithic)	39.2	5.549	8.457	83.5	NREL (11/18)	NREL, Inv. Metamorphic [46]
Perovskite/Si	33.7	1.974	20.99	81.3	JRC/ESTI (5/23)	KAUST, 2-Terminal [42]
Perovskite/Perovskite	29.1	2.154	16.51	81.7	JET (12/22)	NanjiangU/Renshine [47]
Perovskite/Organic	23.6	2.136	14.56	75.56	JET (3/22)	NUS/SERIS, 2-Terminal [48]

Int. Journal of Integrated Engineering Vol. 16 No. 9 (2024) p. 326-338

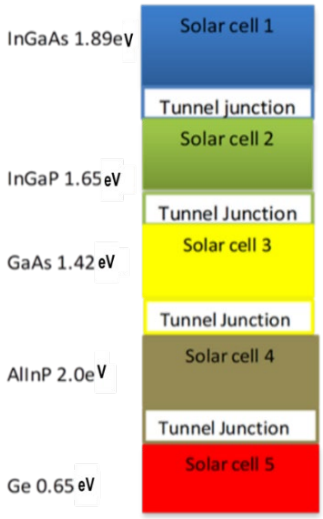

Fig. 1 *The proposed five junction solar module*

By reducing photon recombination and enhancing the generation of photocurrent, interconnect layers play a critical role in increasing the efficiency of multijunction solar cells. AlInP-based window layer is implemented in this proposed design to enhance the performance of the five junction solar cells. Due to the AlInP material's high band gap energy, higher wavelength light can be efficiently absorbed and converted into usable energy. The performance of the multijunction solar cells is improved by this choice of window layer, which also helps to improve photocurrent generation.

2.2 Design Process of Five Junction Solar Modules

Fig. 2 shows the fabrication process of the proposed five-junction solar cells. The top cell in the multijunction solar modules is based on InGaAs, featuring a band gap energy of 1.89 eV, which gives it a blue appearance. This top cell is adept at absorbing shorter wavelength light and enhancing the ejection of electrons from the solar modules. Unlike simple solar cells, where early ejected electrons often dissipate as heat and reduce efficiency, this property significantly boosts the efficiency of multijunction solar modules.

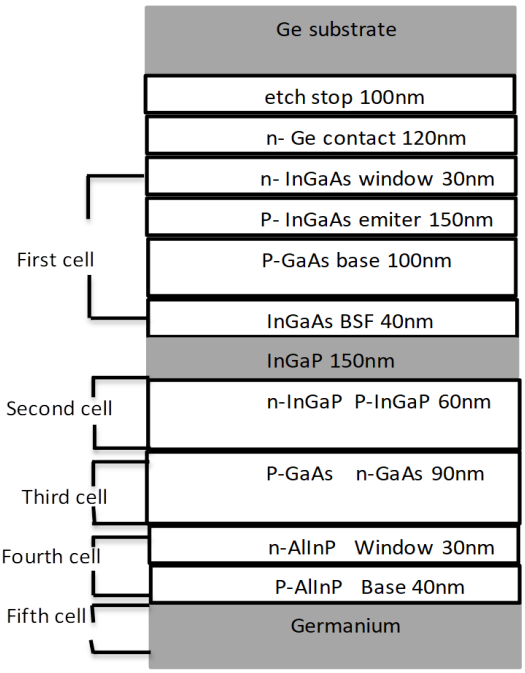

Fig. 2 *Structure of the proposed five junction solar module with window layer and wafer bonding*

The second cell, made from InGaP, has a band gap energy of 1.65 eV and a green colour. It includes a 30 nm thick window layer and itself is 60 nm thick, designed to absorb shorter wavelengths of light. The third cell, utilizing GaAs, displays a yellow colour and is engineered to absorb longer wavelengths. With a band gap energy of 1.424 eV and a thickness of 90 nm, this cell effectively converts a broad spectrum of sunlight into electrical energy.

The fifth junction incorporates AlInP as a grey-coloured window layer with a band gap energy of 2.0 eV, efficiently absorbing longer wavelengths. This 30 nm thick window layer is strategically placed between junctions to regulate electron flow. The final cell, based on germanium, appears red and has a band gap energy of 0.65 eV. Positioned at the bottom of the module, this germanium-based cell absorbs longer wavelengths of light. These carefully selected materials and their strategic placement enhance the overall efficiency of the five-junction solar modules.

3. Mathematical Modelling of Five Junction Solar Module

The performance of multijunction solar modules is assessed by evaluating parameters such as J_{sc}, V_{oc}, fill factor, and efficiency. These parameters are defined and results are obtained using the MATLAB/Simulink model. The J_{sc} for the five-junction solar modules is calculated using Equations (1) and (2). J_{sc} consists of two components, which are dark current and light-generated current (IL). Dark current is the current produced by the p-n junction in the absence of illumination, while IL is generated when the module is exposed to sunlight [23][24][25].

$$\begin{aligned} J_L = {} & J_{sc,1} - J_{0,1}\left[\exp\left(\frac{q(Vi + JLARs, 1}{nKT}\right) - 1\right] + J_{sc,2} - J_{0,2}\left[\exp\left(\frac{q(Vi + JLARs, 1}{nKT}\right) - 1\right] + J_{sc,3} \\ & - J_{0,3}\left[\exp\left(\frac{q(Vi + JLARs, 1}{nKT}\right) - 1\right] + J_{sc,4} - J_{0,4}\left[\exp\left(\frac{q(Vi + JLARs, 1}{nKT}\right) - 1\right] \\ & + J_{sc,5} - J_{0,5}\left[\exp\left(\frac{q(Vi + JLARs, 1}{nKT}\right) - 1\right] \end{aligned} \tag{1}$$

$$Jsc = -JL \tag{2}$$

Equation (3) can be utilized to calculate the V_{oc} of the module. The voltage across the five-junction solar module is at its highest when the current flowing through the PV module is at its minimum.

$$\begin{aligned} V_{oc} = {} & kBT/q[n_1 \ln\left(J_{sc,1} - \frac{Jl}{J_{0,1}} + 1\right) + n_2 \ln\left(J_{sc,2} - \frac{Jl}{J_{0,1}} + 1\right) + n_3 \ln\left(J_{sc,3} - \frac{Jl}{J_{0,1}} + 1\right) \\ & + n_4 \ln\left(J_{sc,4} - \frac{Jl}{J_{0,1}} + 1\right) + n_5 \ln\left(J_{sc,5} - \frac{Jl}{J_{0,1}} + 1\right)] \end{aligned} \tag{3}$$

The fill factor (FF) represents the maximum output power of the solar module FF is the product of the maximum current and voltage. Equation (4) is used to calculate the FF for five a junction solar module in which 0.72 is the constant value for each junction.

$$FF = V_{oc} - \frac{Ln(V_{oc} + 0.72)}{V_{oc}} + 1 \tag{4}$$

The efficiency of the solar PV module is the ratio between the product of maximum PV voltage and maximum PV current to the theoretical maximum power of the module at any irradiance of the sunlight, which can be determined by using the equation (5).

$$\eta = \frac{P_{out}}{P_{in}} = \frac{V_m J_m}{P_{in}} \tag{5}$$

4. Results

4.1 Five Junctions Solar Module

Fig. 3 presents the five-junction solar module modelled in MATLAB/Simulink software. The current-voltage (I-V) characteristic, J_{sc}, V_{oc}, and FF are calculated using the proposed model and the equations presented in Chapter 3. As previously mentioned, the five junctions solar module is capable of absorbing the full spectrum of light in generating electricity with increased efficiency.

Fig. 4 depicts the efficiency of each junction as a function of wavelength. All junctions exhibit an efficiency of 46.7%. The first junction operates within the wavelength range of 300 nm to 400 nm, while the second junction

Int. Journal of Integrated Engineering Vol. 16 No. 9 (2024) p. 326-338

operates within the range of 400 nm to 500 nm. The third junction operates at a wavelength of 700nm, whereas the fourth and fifth junctions operate within the range of 800 nm to 1000 nm. The first junction is particularly responsive to blue light and shorter wavelengths. The second junction, characterized by its green colour, efficiently absorbs and converts green light into electrical energy. The third junction is sensitive to yellow light, while the fourth junction is grey and exhibits sensitivity towards larger wavelengths. Lastly, the last junction, appearing red in colour, effectively absorbs longer wavelengths of sunlight. The efficiency of five junction solar modules is obtained by using the MATLAB/Simulink model where each sub cell produces its current voltage and peak power value according to the wavelength absorption.

Fig. 5 illustrates the characteristic curve of the five junction solar modules under the standard AM1.5 spectrum of sunlight. At the temperature of 25 °C and under the standard spectrum conditions, the voltage is recorded as 2.4 V, and the current is measured at 3.05 A.

Fig. 6 presents the J_{sc} of the five-junction solar module at various levels of irradiances from 400 W/m^2 to 800 W/m^2. With an increase in irradiance from 400 W/m^2 onwards, the J_{sc} value of the five-junction solar module also increases. At an irradiance of 800 W/m^2, the J_{sc} reaches its maximum value of 3.2 mA/cm^2. This peak value is achieved when the sun is at its highest intensity. Subsequently, as the irradiance decreases, the J_{sc} value also decreases accordingly.

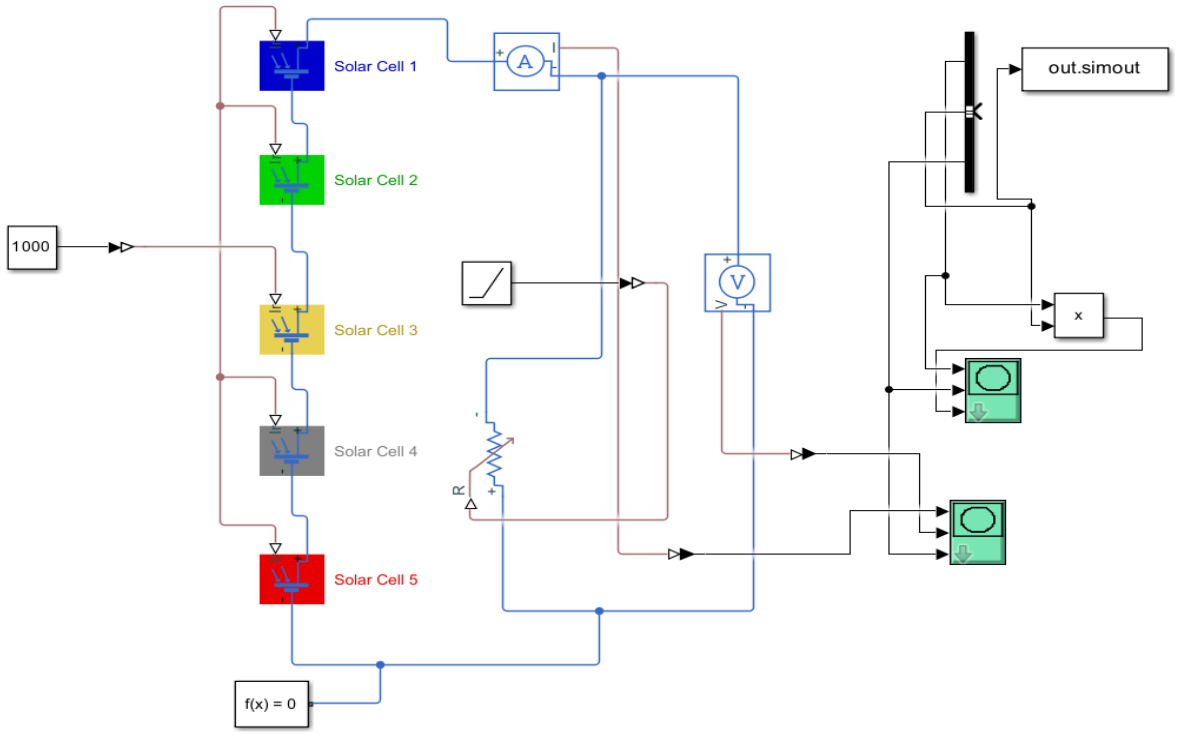

Fig. 3 *MATLAB/Simulink model of the five junctions solar module*

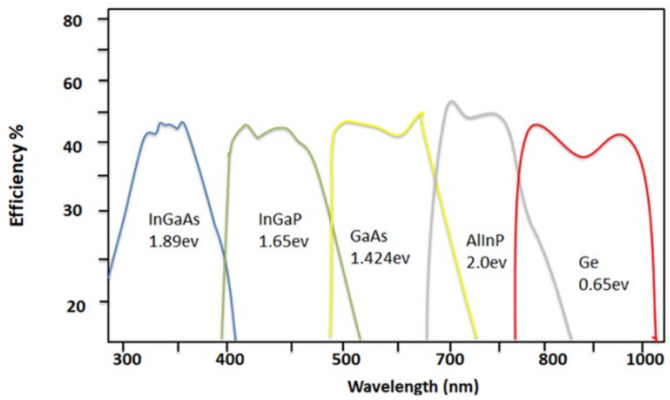

Fig. 4 *Wavelength of light vs efficiency of each junction of the PV module*

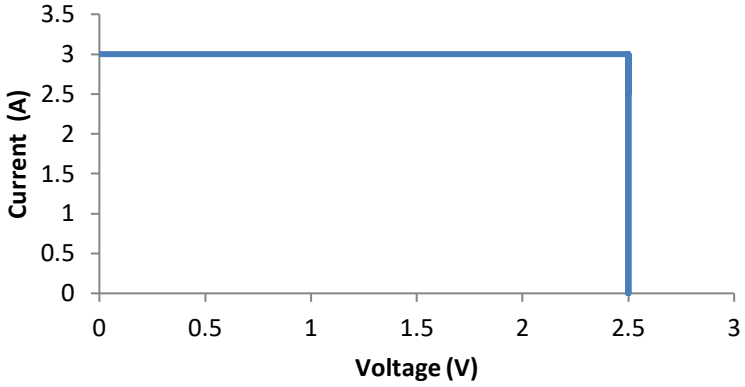

Fig. 5 *Current vs voltage characteristic curve of five junction solar cells*

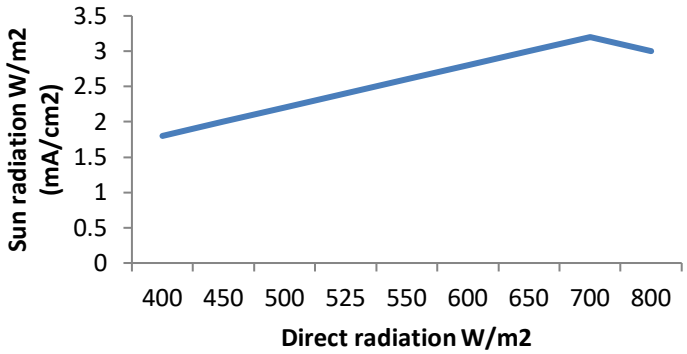

Fig. 6 *Irradiance vs short circuit current of the five junction PV module*

Fig. 7 depicts the relationship between the V_{oc} and irradiance for the five junction solar modules. At an irradiance of 400 W/m^2, the V_{oc} of the solar cell is recorded as 2.44 V. With an increase in the sun's value beyond 400 W/m^2, the V_{oc} of the solar cells also exhibits an upward trend.

The V_{oc} of the solar cells reaches its maximum value at an irradiance of 800 W/m^2, measuring 2.68 V. As the sun intensity decreases beyond this value, the V_{oc} of the five junction solar cells also decreases accordingly. Fig. 8 illustrates the peak power characteristics of the InGaAs, InGaP, GaAs, AlInP, and Ge junctions. At an irradiance of 400 W/m^2, the peak power of the five junction solar cells is recorded as 5.8 W. As the sun's intensity gradually increases, the peak power of the solar cells also increases, reaching its maximum value of 10.5 W at an irradiance of 800 W/m^2. However, as the sun's intensity decreases, the peak power of the solar cells also decreases accordingly.

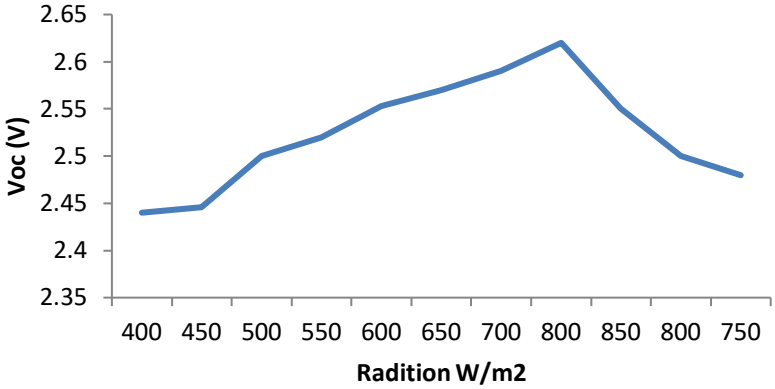

Fig. 7 *Open circuit voltage vs irradiance of sunlight*

Int. Journal of Integrated Engineering Vol. 16 No. 9 (2024) p. 326-338

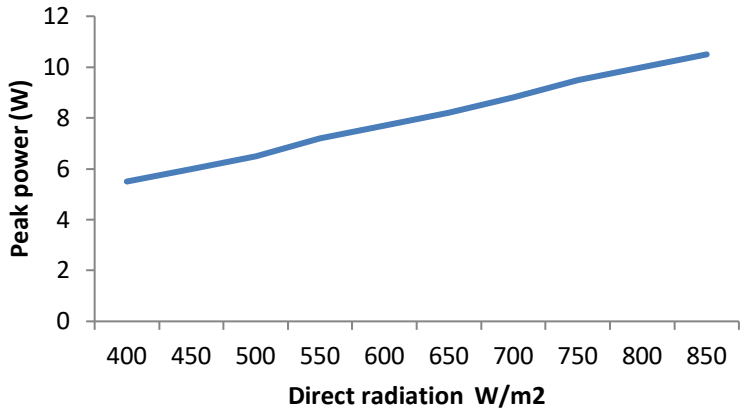

Fig. 8 *Irradiance vs peak power of five junction PV module*

Fig. 9 depicts the FF curve of the five junction solar cells in relation to the solar irradiance. The FF is a measure of the total output power generated by the five junction solar cells, which is the product of the voltage and current. It is influenced by factors such as the J_{sc}, V_{oc}, and peak power of the solar cells.

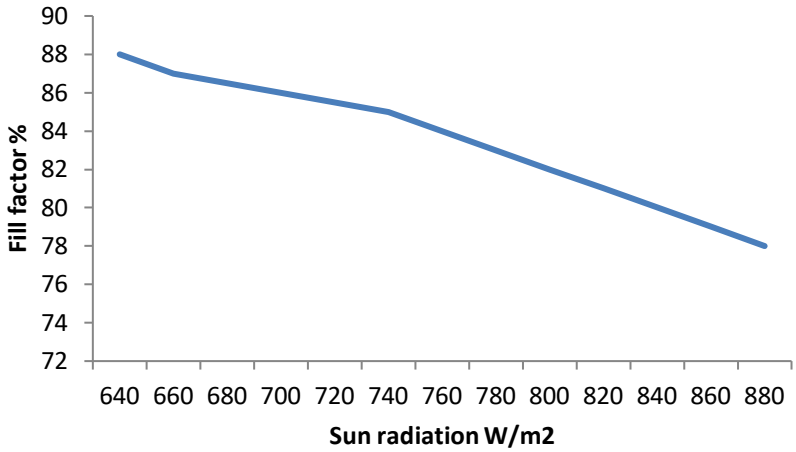

Fig. 9 *Irradiance vs the fill factors of the solar PV*

The FF reaches its peak at 640 W/m², with a maximum value of 90%, indicating the highest efficiency of the solar modules. However, as the irradiance decreases beyond this point, the FF gradually decreases. This reduction in FF is attributed to the decrease in both the J_{sc} and the V_{oc}. During peak daylight hours, the maximum irradiance typically ranges from 700 W/m² to 800 W/m². After this period, as the irradiance decreases, the FF of the PV module also decline accordingly.

The performance of the five junction solar cells was evaluated at the module level under specific conditions, with a temperature of 250 °C and an irradiance of 1000 W/m2. The output characteristics are displayed in Fig. 10. The module has a peak power rating of 220 W, with the J_{sc} of 8 A and the V_{oc} of 37 V.

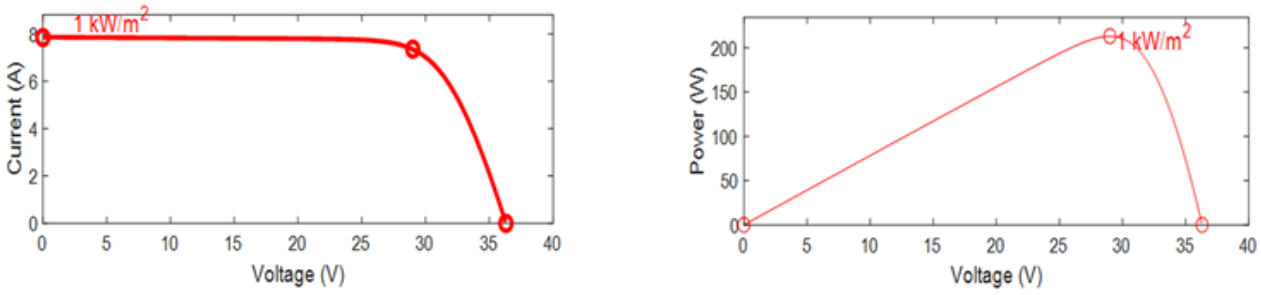

Fig. 10 *Power characteristic curves of five junction solar modules*

4.2 Comparison with Different Number of Solar Cell Junctions

In [26], a study reported an efficiency of 30.40% for triple-junction solar cells using InGaP/GaAs/Ge materials. Table 2 highlights the characteristic properties of these cells, which display low voltage levels and high J_{sc}. These factors can lead to increased heating effects, ultimately reducing overall efficiency. The triple-junction solar cells consist of three sub-cells that absorb specific wavelengths of sunlight, while the unused wavelengths contribute to thermal effects within the module. In [50], the properties of four-junction solar cells are discussed. The study experimentally designed a four-junction solar cells, achieving an overall efficiency of 44.7%. Similarly, in [51], five-junction solar cells are developed, reaching an efficiency of 35.1%. In this case, a GaInNAs lattice mismatch layer is utilized. In the five-junction solar cells used in this work, the inclusion of five sub-cells allows for the absorption of five distinct wavelengths of light, thereby minimizing heating effects and reducing recombination. The design features an AlInP window layer, known for its wide band gap energy, which helps lower recombination and enhance photocurrent generation. Ge is utilized as the substrate for band gap growth, further boosting photocurrent generation by increasing charge carrier production. The sub-cells are both electrically and mechanically connected through wafer bonding. As shown in Table 2, the voltage of the five-junction solar modules exceeds that of the triple-junction solar modules.

Table 2 *Comparison of solar cells with different number of junctions*

Materials	Band gap energy (eV)	V_{oc} (V)	J_{sc} (mA/cm^2)	FF %
Triple junction [26]				
InGaP [26]	1.890	1.4320	16.5000	90.8820
GaAs [26]	1.424	1.0400	28.8001	88.3919
Ge [26]	0.650	0.2210	47.6500	65.6580
Four junction [50]				
GaInP [50]	1.88	1.584	12.42	87.0
GaAs [50]	1.42	1.192	12.60	86.3
GaInAsP [50]	1.12	0.892	12.54	85.0
GaInAs [50]	0.74	0.500	13.69	83.5
Five junction [51]				
AlGaInP [51]	2.10	1.560	3.1	81.4
AlGaInAs [51]	1.70	1.120	2.9	81.2
GaInAs [51]	1.40	0.821	2.4	80.5
GaInNAs [51]	1.00	0.621	1.8	78.0
Ge [51]	0.67	0.321	1.6	75.0
This work				
InGaAs	1.890	3.2	2.65	90
InGaP	1.650	3.0	2.60	90
GaAs	1.424	2.5	2.56	88
AlInP	2.000	2.0	2.54	86
Ge	0.650	1.8	2.45	66

5. Conclusion

The efficiency of existing multijunction solar modules is limited, and this work aims to enhance their efficiency using unique materials with distinct band gap energy values. To achieve this, a five junction solar module is designed, which includes an additional junction to improve efficiency. The specific design presented in this work is based on InGaAs/InGaP/GaAs/AlInP/Ge materials, resulting in a solar module efficiency of 46.7%. The five cells of the solar module are interconnected using wafer bonding techniques, and window layers are incorporated between the cells. Performance testing of the solar cells and module is conducted under conditions of 1000 W/m2 irradiance and a temperature of 25 °C. The irradiance directly impacts the module's performance, with higher intensities leading to improved performance. The output results are obtained through the utilization of a MATLAB/Simulink model. The results clearly demonstrate the enhancement achieved by the five junction solar modules, with the efficiency reaching 46.7%. In the future, the five-junction solar cell's efficiency can be boosted further by introducing an extra lattice mismatch layer. While incorporating additional junctions shows potential for elevating overall solar panel performance, the main hurdle is cost. Current research aims to make multijunction solar cells more affordable, a crucial focus for future development.

Acknowledgement

The research work is financially supported by Universiti Sains Malaysia Short Term Grant 304/PELECT/6315747

Conflict of Interest

Author declared no known conflict of interest.

Author Contribution

The author contributions for this manuscript are as follows: **conceptualization, formal analysis, investigation, methodology, and draft manuscript preparation**: *Muhammad Shehram*; **funding acquisition, project administration, supervision, validation:** *Muhammad Najwan Hamidi;* **review and editing:** *Muhammad Najwan Hamidi, Mohd Khairunaz Mat Desa*; **work co-supervision:** *Aeizaal Azman Abdul Wahab, Mohd Khairunaz Mat Desa*; *All authors reviewed the results and approved the final version of the manuscript*.

References

[1] Li, Ge, Hongbo Lu, Xinyi Li, and Wei Zhang. "Improving the Performance of Direct Bonded Five-Junction Solar Cells by Optimization of AlInP Window Layer." In Photonics, vol. 9, no. 6, p. 404. MDPI, 2022. https://doi.org/10.3390/photonics9060404

[2] Predan, Felix, Oliver Höhn, David Lackner, Alexander Franke, Henning Helmers, and Frank Dimroth. "Development and analysis of wafer-bonded four-junction solar cells based on antimonides with 42% efficiency under concentration." IEEE Journal of Photovoltaics 10, no. 2 (2019): 495-501. https://doi.org/10.1109/JPHOTOV.2019.2957663

[3] Yamaguchi, Masafumi, Frank Dimroth, John F. Geisz, and Nicholas J. Ekins-Daukes. "Multi-junction solar cells paving the way for super high efficiency." Journal of Applied Physics 129, no. 24 (2021): 240901. https://doi.org/10.1063/5.0048653

[4] Hoehn, Oliver, Markus Niemeyer, Charlotte Weiss, David Lackner, Felix Predan, Alexander Franke, Paul Beutel et al. "Development of Germanium-based wafer-bonded four-junction solar cells." IEEE Journal of Photovoltaics 9, no. 6 (2019): 1625-1630. https://doi.org/10.1109/JPHOTOV.2019.2941770

[5] Lombardero, Iván, Luis Cifuentes, Mercedes Gabás, and Carlos Algora. "Manufacturing process for III–V multijunction solar cells on germanium substrates with a total thickness below 60 microns." Progress in Photovoltaics: Research and Applications 30, no. 7 (2022): 740-749. https://doi.org/10.1002/pip.3547

[6] Weiss, Charlotte, Jonas Schön, Oliver Höhn, Christian Mohr, Rufi Kurstjens, Bruno Boizot, and Stefan Janz. "Potential analysis of a rear-side passivation for multi-junction space solar cells based on germanium substrates." In 2018 IEEE 7th World Conference on Photovoltaic Energy Conversion (WCPEC) (A Joint Conference of 45th IEEE PVSC (Photovoltaics Specialists Conference), 28th PVSEC & 34th EU PVSEC), pp. 3392-3396. IEEE, 2018. https://doi.org/10.1109/PVSC.2018.8547334

[7] Strandberg, Rune. "An analytic approach to the modeling of multijunction solar cells." IEEE Journal of Photovoltaics 10, no. 6 (2020): 1701-1711. https://doi.org/10.1109/JPHOTOV.2020.3013974

[8] Kotamraju, Siva, M. Sukeerthi, Suresh E. Puthanveettil, and M. Sankaran. "Study of degradation in InGaP/InGaAs/Ge multi-junction solar cell characteristics due to irradiation-induced deep level traps using finite element analysis." Solar Energy 178 (2019): 215-221. https://doi.org/10.1016/j.solener.2018.12.036

[9] Peters, Ian Marius, Carlos David Rodríguez Gallegos, Larry Lüer, Jens A. Hauch, and Christoph J. Brabec. "Practical limits of multijunction solar cells." Progress in Photovoltaics: Research and Applications (2022).

[10] Hou, GuoJiao, Iván García, and Ignacio Rey-Stolle. "High-low refractive index stacks for broadband antireflection coatings for multijunction solar cells." Solar Energy 217 (2021): 29-39.

[11] Arzbin, Hamid Reza, and Abbas Ghadimi. "Improving the performance of a multi-junction solar cell by optimizing BSF, base and emitter layers." Materials Science and Engineering: B 243 (2019): 108-114.

[12] Devendra, K. C., D. K. Shah, R. Wagle, A. Shrivastava, and D. Parajuli. "Ingap window layer for gallium arsenide (Gaas) based solar cell using pc1d simulation." J. Adv. Res. Dyn. Control Syst 12, no. 7 (2020): 2878-2885.

[13] Dai, Pan, Wenxian Yang, Junhua Long, Ming Tan, Yuanyuan Wu, Shiro Uchida, Lifeng Bian, and Shulong Lu. "The investigation of wafer-bonded multi-junction solar cell grown by MBE." Journal of Crystal Growth 515 (2019): 16-20.

[14] Lu, Shulong, and Shiro Uchida. "Room-Temperature Wafer Bonded Multi-Junction Solar Cell Grown by Solid State Molecular Beam Epitaxy." MRS Advances 1 (2016): 2907-2916.

[15] Oshima, Ryuji, Yuki Ishitsuka, Yoshinobu Okano, and Takeyoshi Sugaya. "Comparison of different passivation layers for GaInAs solar cells grown by solid-source molecular beam epitaxy." Journal of Crystal Growth 593 (2022): 126769.

[16] Takahashi, Kazuya, Ryoji Shinoda, Syun Mitsufuji, Motoaki Iwaya, Satoshi Kamiyama, Tetsuya Takeuchi, Tomokazu Hattori, Isamu Akasaki, and Hiroshi Amano. "Fabrication of a GaInN/GaInP/GaInAs/Ge four-junction solar cell using the wafer bonding technology." Japanese Journal of Applied Physics 58, no. 7 (2019): 072003.
[17] Baiju, Adil, and Maksym Yarema. "Status and challenges of multi-junction solar cell technology." Frontiers in Energy Research 10 (2022).
[18] Barrutia, Laura, Iván García, Enrique Barrigón, Mario Ochoa, Carlos Algora, and Ignacio Rey-Stolle. "Impact of the III-V/Ge nucleation routine on the performance of high efficiency multijunction solar cells." Solar Energy Materials and Solar Cells 207 (2020): 110355.
[19] Sharma, Divya, Rajesh Mehra, and Balwinder Raj. "Methods for integration of III-V compound and silicon multijunction solar cell." In International Conference on Emerging Technologies: AI, IoT and CPS for science and technology applications, Dept. of ECE, NITTTR Chandigarh, pp. 6-7. 2021.
[20] Yamaguchi, Masafumi, Frank Dimroth, Nicholas J. Ekins-Daukes, Nobuaki Kojima, and Yoshio Ohshita. "Overview and loss analysis of III–V single-junction and multi-junction solar cells." EPJ Photovoltaics 13 (2022): 22.
[21] Chawla, Rashmi, Poonam Singhal, and Amit Kumar Garg. "Design and analysis of multi junction solar photovoltaic cell with graphene as an intermediate layer." Journal of nanoscience and nanotechnology 20, no. 6 (2020): 3693-3702.
[22] Di Carlo Rasi, Dario, and René AJ Janssen. "Advances in solution-processed multijunction organic solar cells." Advanced Materials 31, no. 10 (2019): 1806499.
[23] Wang, Zilong, Hua Zhang, Binlin Dou, Guanhua Zhang, and Weidong Wu. "Theoretical and experimental evaluation on the electrical properties of multi-junction solar cells in a reflective concentration photovoltaic system." Energy Reports 8 (2022): 820-831.
[24] Al-Ezzi, Athil S., and Mohamed Nainar M. Ansari. "Photovoltaic Solar Cells: A Review." Applied System Innovation 5, no. 4 (2022): 67.
[25] Wang, Zilong, Hua Zhang, Binlin Dou, Weidong Wu, and Guanhua Zhang. "Numerical and experimental research of the characteristics of concentration solar cells." Frontiers in Energy 15 (2021): 279-291.
[26] Hadjdida, Abdelkader, Mohamed Bourahla, H. Bülent Ertan, and Mohamed Bekhti. "Analytical modelling, simulation and comparative study of multi-junction solar cells efficiency." International Journal of Renewable Energy Research 8, no. 4 (2018): 1824-1832.
[27] Li, Deng-Bing, Sandip S. Bista, Rasha A. Awni, Sabin Neupane, Abasi Abudulimu, Xiaoming Wang, Kamala K. Subedi et al. "20%-efficient polycrystalline Cd (Se, Te) thin-film solar cells with compositional gradient near the front junction." Nature Communications 13, no. 1 (2022): 7849.
[28] Lin, Hao, Miao Yang, Xiaoning Ru, Genshun Wang, Shi Yin, Fuguo Peng, Chengjian Hong et al. "Silicon heterojunction solar cells with up to 26.81% efficiency achieved by electrically optimized nanocrystalline-silicon hole contact layers." Nature Energy 8, no. 8 (2023): 789-799.
[29] Paulauskas, Tadas, Vaidas Pačebutas, Viktorija Strazdienė, Andrejus Geižutis, Jan Devenson, Mindaugas Kamarauskas, Martynas Skapas et al. "Performance assessment of a triple-junction solar cell with 1.0 eV GaAsBi absorber." Discover Nano 18, no. 1 (2023): 86.
[30] Peters, Ian Marius, Carlos David Rodríguez Gallegos, Larry Lüer, Jens A. Hauch, and Christoph J. Brabec. "Practical limits of multijunction solar cells." Progress in Photovoltaics: Research and Applications 31, no. 10 (2023): 1006-1015.
[31] Wang, Rongbo, Meidouxue Han, Ya Wang, Juntao Zhao, Jiawei Zhang, Yi Ding, Ying Zhao, Xiaodan Zhang, and Guofu Hou. "Recent progress on efficient perovskite/organic tandem solar cells." Journal of Energy Chemistry 83 (2023): 158-172.
[32] Heydarian, Maryamsadat, Minasadat Heydarian, Alexander J. Bett, Martin Bivour, Florian Schindler, Martin Hermle, Martin C. Schubert, Patricia SC Schulze, Juliane Borchert, and Stefan W. Glunz. "Monolithic Two-Terminal Perovskite/Perovskite/Silicon Triple-Junction Solar Cells with Open Circuit Voltage> 2.8 V." ACS Energy Letters 8, no. 10 (2023): 4186-4192.
[33] Kharchich, Fatima Zahra, and Abdellatif Khamlichi. "Optimizing efficiency of InGaP/GaAs dual-junction solar cells with double tunnel junction and bottom back surface field layers." Optik 272 (2023): 170196.
[34] Karim, Md Ehsanul, and Abu SM Mohsin. "Metasurface absorber based single junction thin film solar cell exceeding 30% efficiency." Optics Express 32, no. 5 (2024): 8214-8229.
[35] Liu, Siyi, Yong Qian, Yinyue Lin, Lijie Sun, Yongxin Zhu, and Dongdong Li. "Multilayer anti-reflective coating with ultra-low refractive index SiO2 nanopillars for high efficiency multi-junction GaAs solar cells." Solar Energy Materials and Solar Cells 266 (2024): 112679.
[36] Nieto, Luis M. Nieto, Juan P. Ferrer Rodríguez, Raúl Mata Campos, and Pedro J. Pérez Higueras. "Multi-junction solar cell measurements at ultra-high irradiances for different temperatures and spectra." Solar Energy Materials and Solar Cells 266 (2024): 112651.
[37] Hu, Yi, Benyuan Chen, and Peng Xu. "A comprehensive simulation study of multi-junction solar cell." Materials Research Express 11, no. 5 (2024): 056201.

[38] Matsui, Takuya, Adrien Bidiville, Keigou Maejima, Hitoshi Sai, Takashi Koida, Takashi Suezaki, Mitsuhiro Matsumoto, Kimihiko Saito, Isao Yoshida, and Michio Kondo. "High-efficiency amorphous silicon solar cells: impact of deposition rate on metastability." Applied Physics Letters 106, no. 5 (2015).
[39] Qarony, Wayesh, Mohammad I. Hossain, M. Khalid Hossain, M. Jalal Uddin, A. Haque, A. R. Saad, and Yuen Hong Tsang. "Efficient amorphous silicon solar cells: characterization, optimization, and optical loss analysis." Results in physics 7 (2017): 4287-4293.
[40] Sai, Hitoshi, Takuya Matsui, Hideo Kumagai, and Koji Matsubara. "Thin-film microcrystalline silicon solar cells: 11.9% efficiency and beyond." Applied Physics Express 11, no. 2 (2018): 022301.
[41] Green, Martin, Ewan Dunlop, Jochen Hohl-Ebinger, Masahiro Yoshita, Nikos Kopidakis, and Xiaojing Hao. "Solar cell efficiency tables (version 57)." Progress in photovoltaics: research and applications 29, no. 1 (2021): 3-15.
[42] Wanlass, Mark. Systems and methods for advanced ultra-high-performance InP solar cells. No. 9,590,131. National Renewable Energy Laboratory (NREL), Golden, CO (United States), 2017.
[43] Zhu, Lei, Ming Zhang, Jinqiu Xu, Chao Li, Jun Yan, Guanqing Zhou, Wenkai Zhong et al. "Single-junction organic solar cells with over 19% efficiency enabled by a refined double-fibril network morphology." Nature Materials 21, no. 6 (2022): 656-663.
[44] Ren, Yameng, Dan Zhang, Jiajia Suo, Yiming Cao, Felix T. Eickemeyer, Nick Vlachopoulos, Shaik M. Zakeeruddin, Anders Hagfeldt, and Michael Grätzel. "Hydroxamic acid pre-adsorption raises the efficiency of cosensitized solar cells." Nature 613, no. 7942 (2023): 60-65.
[45] Geisz, John F., Myles A. Steiner, Nikhil Jain, Kevin L. Schulte, Ryan M. France, William E. McMahon, Emmett E. Perl, and Daniel J. Friedman. "Building a six-junction inverted metamorphic concentrator solar cell." IEEE Journal of Photovoltaics 8, no. 2 (2017): 626-632.
[46] Lin, Renxing, Jian Xu, Mingyang Wei, Yurui Wang, Zhengyuan Qin, Zhou Liu, Jinlong Wu et al. "All-perovskite tandem solar cells with improved grain surface passivation." Nature 603, no. 7899 (2022): 73-78.
[47] Chen, Wei, Yudong Zhu, Jingwei Xiu, Guocong Chen, Haoming Liang, Shunchang Liu, Hansong Xue et al. "Monolithic perovskite/organic tandem solar cells with 23.6% efficiency enabled by reduced voltage losses and optimized interconnecting layer." Nature Energy 7, no. 3 (2022): 229-237.
[48] Shockley, William, and Hans Queisser. "Detailed balance limit of efficiency of p–n junction solar cells." In Renewable energy, pp. Vol2_35-Vol2_54. Routledge, 2018.
[49] Shehram, Muhammad, Muhammad Najwan Hamidi, Aeizaal Azman A. Wahab, and MK Mat Desa. "Modeling of Multijunction Solar Cells InGaAs/InGaP/GaAs/GeSi for Improving the Efficiency of PV Modules by 43%." In International Conference on Robotics, Vision, Signal Processing and Power Applications, pp. 35-41. Singapore: Springer Nature Singapore, 2021.
[50] Dimroth, Frank, Matthias Grave, Paul Beutel, Ulrich Fiedeler, Christian Karcher, Thomas ND Tibbits, Eduard Oliva et al. "Wafer bonded four-junction GaInP/GaAs//GaInAsP/GaInAs concentrator solar cells with 44.7% efficiency." Progress in Photovoltaics: Research and Applications 22, no. 3 (2014): 277-282.
[51] Chen, Bing-zhen, Yang Zhang, Qing Wang, and Zhi-yong Wang. "Photoelectric Property Improvement of 1.0-eV GaInNAs and Applications in Lattice-Matched Five-Junction Solar Cells." Chinese Physics Letters 35, no. 7 (2018): 078801.